

## Correlations and scaling in one-dimensional heat conduction

J. M. Deutsch and Onuttom Narayan

*Department of Physics, University of California, Santa Cruz, California 95064, USA*

(Received 12 June 2003; published 14 October 2003)

We examine numerically the full spatiotemporal correlation functions for all hydrodynamic quantities for the random collision model introduced recently. The autocorrelation function of the heat current, through the Kubo formula, gives a thermal conductivity exponent of  $1/3$  in agreement with the analytical prediction and previous numerical work. Remarkably, this result depends crucially on the choice of boundary conditions: for periodic boundary conditions (as opposed to open boundary conditions with heat baths) the exponent is  $\approx 1/2$ . All primitive hydrodynamic quantities scale with the dynamic critical exponent predicted analytically.

DOI: 10.1103/PhysRevE.68.041203

PACS number(s): 44.10.+i, 05.10.Ln, 75.40.Mg

### I. INTRODUCTION

Heat conduction in one-dimensional systems is a simple example of the general problem of singular transport coefficients [1]. Apart from this theoretical significance, there is increasing experimental relevance due to the tremendous advances in nanotube technology [2,3], and the importance of understanding their thermal properties. It appears that the thermal conductivity  $\kappa(L)$ , as a function of the system size  $L$ , diverges with increasing  $L$  for one-dimensional momentum conserving systems [4–7]. Recently [7], a hydrodynamic description has been proposed, which obtained the analytic prediction of

$$\kappa(L) \sim L^{1/3} \quad (1)$$

for such momentum conserving systems [5,7]. Numerical results on various systems [5,6], most recently work on Sinai and Chernov's pencease model [8] and the random collision (RC) model [9], confirm this prediction.

Despite the numerical confirmation, there is reason to investigate the analytical predictions further. The hydrodynamic description makes detailed predictions about the dynamical behavior of all conserved quantities in the system: energy, momentum, and mass. The heat conductivity is only a single, and rather indirect, verification of the theoretical picture. In addition, there are significant corrections to the scaling form predicted for  $\kappa(L)$ , so that it is appropriate to explore whether they are indeed simply corrections to scaling for small  $L$ , or reflect a departure from the hydrodynamic description. Finally, the connection between conductivity and correlation functions through the Kubo formula [10], examined briefly in our earlier paper, is worth further examination.

In this paper, we study the RC model [9], which was recently introduced for one-dimensional transport, and numerically obtain the full spatiotemporal form of all correlation functions between the conserved hydrodynamic variables. We find both propagating and dispersive modes with a dispersion relation in agreement with the analytical result.

The autocorrelation function of the heat current, which can be obtained in terms of the primitive hydrodynamic quantities has a spatiotemporal structure that is not amenable to any simple scaling description for length and time scales much larger than (about thirty times) the interparticle spacing

and collision time. However, as we will argue, the existence of larger corrections to scaling for the heat current is perhaps not surprising. Moreover, the continuity relation connects the heat current to the primitive hydrodynamic quantities, so these corrections must vanish on suitably large length and time scales. In accordance with this expectation, the autocorrelation function of the total heat current (integrated over the entire system),  $C_{JJ}(t)$ , is much better behaved. The integral

$$I(t) \equiv \frac{1}{L} \int_0^t dt' C_{JJ}(t') \quad (2)$$

scales with  $t$  with an exponent close to  $1/3$ , although depending on the model parameters chosen  $L$  can be as large as  $\sim 10\,000$  before the asymptotic scaling behavior is seen.

The autocorrelation function  $C_{JJ}(t)$  was measured with two different boundary conditions: open boundary conditions with heat baths at the ends and periodic boundary conditions. In both cases,  $I(t)$  looks the same at short times, and has oscillatory behavior for  $t \sim L$ . For open boundary conditions, the oscillations damp out rapidly, and therefore asymptote on a time scale  $\sim L$ , as assumed in the analytical treatment. Thus  $I(t \rightarrow \infty)$ , which is connected to the conductivity through the Kubo formula, scales as  $\sim L^{1/3}$ . On the other hand, with periodic boundary conditions,  $I(t)$  continues to grow after the oscillations set in, and  $I(\infty) \sim L^{1/2}$ . This dependence on boundary conditions, although highly unusual, is consistent with the analytical picture: the dynamical exponent of  $3/2$  would normally convert a  $t^{1/3}$  scaling to  $L^{1/2}$ , but with open boundary conditions the cutoff to the time integral is set by the modes propagating to the heat baths at the ends, i.e., at  $t$  of  $O(L)$ .

### II. EARLIER RESULTS

A large number of systems with dimension  $d=1$  have been analytically [11–13] or numerically [2,5,6,13,14] found to have a singular heat conductivity,  $\kappa(L) \sim L^\alpha$  with  $\alpha > 0$ . Various values of  $\alpha$  have been obtained for different models. Positive values of  $\alpha$  are seen either when a model is integrable, when the value of  $\alpha$  depends on the details of the model, or when the interparticle interactions in the model are momentum conserving.

For any nonintegrable system, it is possible to construct a

hydrodynamic description, where it is assumed that local thermal equilibrium is reached [7,15]. Since long range order is precluded in  $d=1$ , the hydrodynamic description is only in terms of conserved quantities: energy, number, and (when momentum is conserved) momentum densities. This is the standard hydrodynamic treatment of a normal fluid. There are two propagating sound modes and a diffusive mode for heat transport. The addition of thermal noise to the hydrodynamic equations leads to singular corrections when  $d < 2$ . The spreading of a sound pulse is now superdiffusive: the width  $l$  is related to time  $t$  as  $l \sim t^{2/3}$ , with a dynamic exponent  $z$  exactly equal to  $3/2$  for  $d=1$ . The heat diffusion mode is no longer diffusive: contributions to the heat current that are propagating and bilinear in the primitive hydrodynamic densities, that are inconsequential for  $d > 2$ , dominate (for long wavelength and low frequency) for  $d=1$ . The autocorrelation function of the heat current decays as  $C_{JJ}(t) \sim t^{-2/3}$ . If one integrates this function, with open boundary conditions and heat baths, the propagating nature of the modes cuts off the integral  $I(t)$  at  $t$  of  $O(L)$ . Using the Kubo formula, one obtains  $\kappa(L) \sim L^\alpha$  with  $\alpha = 1/3$ .

### III. THE MODEL

There have been numerical studies of heat conduction in various one-dimensional models [2,5,6,13,14]. One of the simplest such models is that of a chain of point particles undergoing one-dimensional elastic collisions with heat baths at the two ends of the chain. The drawback of this model is that it is not chaotic [5]; in fact, when the particles in the chain are all of equal mass, the model is integrable. As explained in the preceding section, the hydrodynamic description that yields a universal value of  $\alpha = 1/3$  is only valid if the system reaches local thermal equilibrium. Even when the masses of the particles in the chain alternate,  $\alpha$  is found to converge very slowly towards its asymptotic value, requiring system sizes of  $\sim 16\,000$  or larger.

To alleviate this problem, we recently introduced the RC model [9]. This can be viewed as the limit of rough particles confined to a narrow tube, with the width of the tube sufficiently small so that particles cannot pass each other, in the limit that the size of the particles (and the width of the tube) approach zero. In this limit, the particles move along a one-dimensional line, but possess longitudinal as well as transverse momentum, both of which contribute to the particle energy. Interparticle collisions are elastic. Owing to the roughness of the particles, particles emerge from a collision with random momenta (respecting energy momentum conservation and detailed balance). The transverse degree of freedom effectively serves as a random source/sink of longitudinal kinetic energy in any collision, while strictly maintaining conservation of total energy. The extra randomization introduced by the transverse momentum is expected to equilibrate the system much more effectively. Numerically, the conductivity  $\kappa(L)$  is found to scale much better, with  $L^\alpha$  scaling observed for  $L \sim 100-1000$ . However, depending on the particle masses in the model, there is a slight variation in the measured  $\alpha$ , with  $\alpha = 0.28$  when all the particles have the same mass, and  $\alpha = 0.33$  when the particle masses alternate

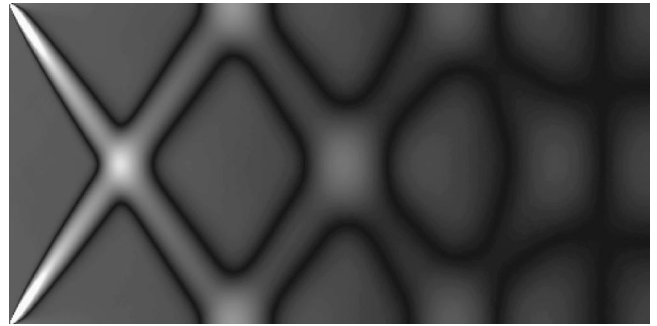


FIG. 1. Grayscale plot of the autocorrelation function of the momentum density,  $C_{vv}(x,t)$ . The vertical and horizontal directions are  $x$  and  $t$ , respectively. Periodic boundary conditions are used for the  $x$  direction. The length of the system is  $L=512$ . The bright regions correspond to intensity peaks, and clearly show the propagating sound modes.

with a mass ratio of 2.62. This indicates that corrections to the asymptotic scaling form, although much reduced, have not been completely eliminated.

### IV. SPATIOTEMPORAL CORRELATIONS

In this section, we present numerical results for the spatiotemporal dependence of the correlation functions of the primitive hydrodynamic densities: energy, momentum, and number. The motivation for carrying out this study has been discussed at the beginning of this paper.

Figure 1 shows the autocorrelation function of the momentum density,  $C_{vv}(x,t)$ , as a function of position  $x$  and time  $t$ . The size of the system is  $L=512$ , all particles have unit mass, and periodic boundary conditions in  $x$  are used. One can clearly see two pulses propagating in opposite directions at constant speed, corresponding to the two sound modes. Even when the pulses collide with each other, they emerge essentially unaffected. The figure also shows a slight broadening of the pulses as  $t$  is increased. To make this picture quantitative, Fig. 2 plots  $C_{vv}(x,t)$  as a function of  $x$  for various values of  $t$ .

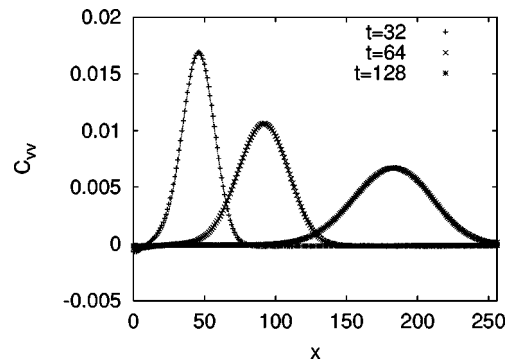


FIG. 2. Autocorrelation function of the momentum density,  $C_{vv}(x,t)$ , as a function of  $x$  for  $t=32, 64$ , and  $128$ . Periodic boundary conditions are used for  $x$ , and the length of the system is  $L=512$ . Since  $C_{vv}$  is symmetric in  $x$ , only  $x > 0$  is shown. As is shown in the figure, the data fit a Gaussian form excellently, propagating outwards at constant speed and broadening as  $\sim t^{2/3}$ .

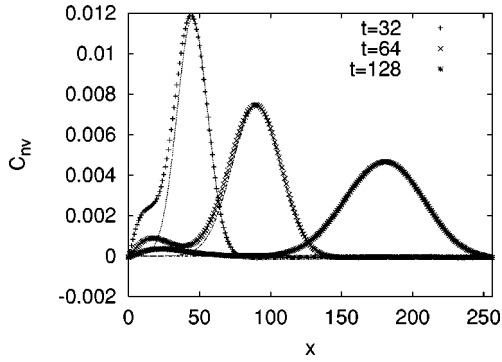


FIG. 3. Cross-correlation function of the mass and momentum density,  $C_{nv}(x,t)$ , as a function of  $x$  for  $t=32, 64,$  and  $128$ . Periodic boundary conditions are used for  $x$ , and the length of the system is  $L=512$ . Only  $x>0$  is shown, since the function is antisymmetric. The large propagating peak, corresponding to the sound mode, is fitted to a Gaussian in the figure. The bump near the origin comes from the heat mode, and has not been fitted.

The lines going through the data points are fits to the functional form  $C_{vv}(x,t) = (A/t^{2/3}) \exp[-B(x-ct)^2/t^{4/3}]$ , with  $A, B,$  and  $c$  as fitting parameters that are independent of  $t$  [16]. The fitting form works surprisingly well. Although for spatial dimension  $d>2$  one indeed expects a propagating Gaussian pulse, for  $d<2$  the scaling theory only predicts that the pulse should spread out as  $\sim t^{2/3}$ , and does not require a Gaussian form.

Similar results are shown in Fig. 3 for the cross-correlation function of the number and momentum densities,  $C_{nv}(x,t)$ .

Figure 4 shows the autocorrelation function for the number density,  $C_{nn}(x,t)$ . In addition to the propagating parts, one can see a peak near the origin. This peak comes from the heat transport mode, which is diffusive for  $d>2$ . The same structure is observed in the autocorrelation function for the energy density,  $C_{ee}(x,t)$ .

In order to extract the heat transport mode, suppressing the sound modes, in Fig. 5 we plot  $C_{qq}(x,t)$ , the autocorrelation function of

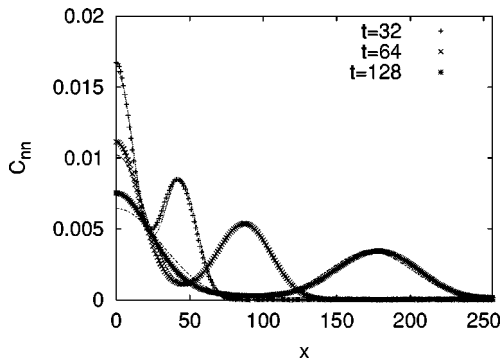


FIG. 4. Autocorrelation function of the mass density,  $C_{nn}(x,t)$ , as a function of  $x$  for  $t=32, 64,$  and  $128$ . Periodic boundary conditions are used for  $x$ , and the length of the system is  $L=512$ . The function is fitted to the sum of a propagating and diffusing Gaussian with the width of both scaling as  $\sim t^{2/3}$ . The second peak does not fit as well as the first one; as discussed in the text, the corrections to scaling for this peak are expected to be much stronger.

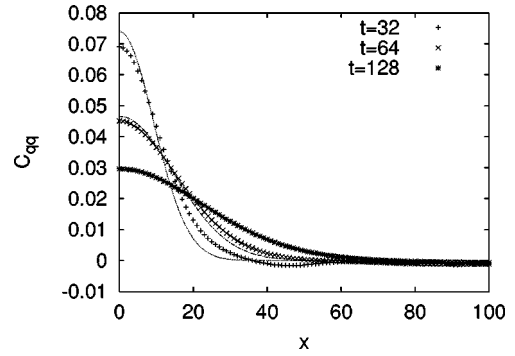


FIG. 5. Autocorrelation function for the heat transport mode. Periodic boundary conditions are used for  $x$ , and the length of the system is  $L=512$ . Comparing with  $C_{nn}(x,t)$  one can see that the sound peak has been eliminated. The fit shown in the figure is to a diffusing form: a Gaussian that is centered at the origin, spreading out as  $t^{2/3}$ . The fit is only approximate, as was the case for the peak at the origin for  $C_{nn}$  in Fig. 4.

lation function of

$$q(x,t) = e(x,t) - (\bar{h}/\bar{n})n(x,t), \quad (3)$$

where  $\bar{h}$  and  $\bar{n}$  are the spatially averaged enthalpy and number density, respectively. At long wavelengths and low frequencies, this corresponds to the heat transport mode [15]. The peak broadens with time with a width  $\sim t^{2/3}$ , but the fit is not as good as for the previous plots.

The scaling of  $C_{qq}(x,t)$  requires careful consideration for  $d<2$ . The hydrodynamic equation for  $q(x,t)$  is

$$\partial_t q + \nabla \cdot (v \delta q + v a \delta e) = \kappa_0 \nabla^2 T + O(v^2), \quad (4)$$

where  $\kappa_0$  is the bare heat conductivity,  $T$  is the temperature,  $\delta q$  and  $\delta e$  are the deviations of  $q$  and  $e$  from their average values, and  $a = \bar{h}/\bar{e} - 1$ . (For the RC model,  $a=1$ .) When fluctuations around average values are small, the second term on the left-hand side of Eq. (4) is second order in the fluctuating fields and can be neglected, yielding diffusive transport for  $q$ . However, for  $d<2$ , one can see [7] that this advective contribution to the heat current,  $v \delta q + v a \delta e$ , dominates at long wavelengths and low frequencies. Thus one expects  $q$  to propagate, with the propagating behavior becoming increasingly important at long length and time scales. This propagating behavior was used in Ref. [7] to argue for a cutoff of  $t \sim L$  for correlations in a system of size  $L$  with heat baths at the ends. We will discuss this issue further in the following section.

## V. HEAT CURRENT

We have seen in the preceding section that the conserved hydrodynamic quantities satisfy the predictions of the scaling theory: two propagating modes which disperse according to  $\delta x \sim t^{2/3}$ , and a heat transport mode. We have also seen that the third mode, unlike for  $d>2$ , is not a simple diffusing mode. We now turn to the autocorrelation function of the heat current. For momentum conserving systems, it can be

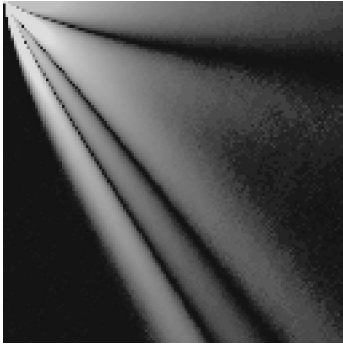


FIG. 6. Grayscale plot of the autocorrelation function of the heat current,  $C_{jj}(x,t)$ . The vertical and horizontal directions are  $x$  and  $t$ , respectively. Periodic boundary conditions are used for the  $x$  direction. The length of the system is  $L=512$ . The intensity peaks move out linearly from  $x=0$  as a function of time.

shown on very general grounds [17] that this is the correlation function that is related to the thermal conductivity through the Kubo formula [10].

Figure 6 shows a grayscale plot (nonlinear, to enhance clarity) of the autocorrelation function of the heat current,  $C_{jj}(x,t)$ , similar to that for  $C_{vv}$  shown in the preceding section. The current  $j(x,t)$  is defined as

$$j(x,t) = \sum_i \delta(x_i - x) v_i [\epsilon_i - (\bar{h}/\bar{n})], \quad (5)$$

where the sum is over particles and  $\epsilon_i$  is the energy of the  $i$ th particle.  $j(x,t)$  is the current that corresponds to  $q$ ; its hydrodynamic form can be obtained from Eq. (4) as

$$j(x,t) = v[\delta q + \delta \epsilon] - \kappa_0 \nabla T + O(v^2). \quad (6)$$

The propagating nature of the heat current can be seen by following the intensity peaks in the figure; the range in time over which this can be seen is not as large as for  $C_{vv}$ , because  $C_{jj}$  decays much faster. As in the preceding section, Fig. 7 shows  $C_{jj}$  as a function of  $x$  for different values of  $t$ .

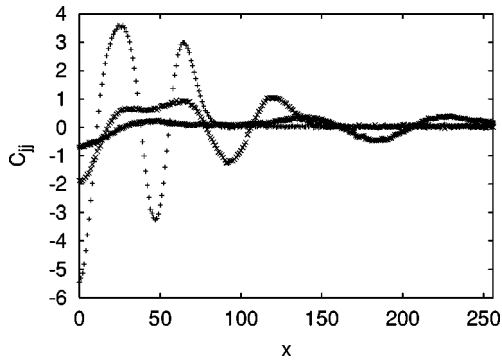


FIG. 7. Autocorrelation function of the heat current,  $C_{jj}(x,t)$ , as a function of  $x$  for  $t=32, 64,$  and  $128$ . Periodic boundary conditions are used for  $x$ , and the length of the system is  $L=512$ . The peaks decay, broaden, and shift outwards as a function of time. No simple scaling form fits the data.

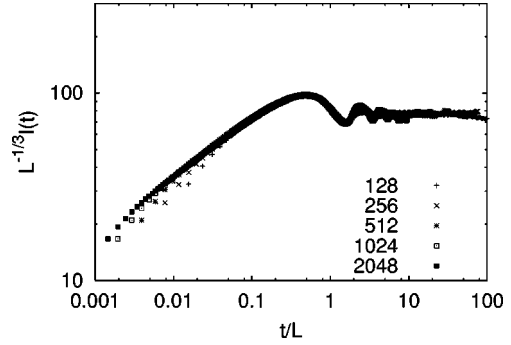


FIG. 8. Log-log plot of  $I(t)/L^{1/3}$  vs  $t/L$  for systems of different lengths, where  $I(t)$  is defined in Eq. (2). The particle masses alternate between 1 and 2.62. Open boundary conditions with heat baths at the two ends are used. The data show a good scaling collapse, indicating that  $I(\infty) \sim L^{1/3}$ .

Although the peaks shift outwards and broaden with time, unfortunately no clear scaling of any form can be seen at small  $t$ . This result might seem disturbing, since the values of  $t$  in Fig. 7, though not large, are sufficient to see good scaling in the basic conserved quantities, as shown in the preceding section. However, as seen in Eq. (6), the hydrodynamic form of the current has advective contributions that are bilinear in the primitive conserved quantities, which dominate at long length and time scales, and other dissipative contributions as well. In a diagrammatic field theoretic expansion, one expects relatively larger contributions from short wavelength modes, aggravated by the fact that although the first term on the right-hand side of Eq. (6) dominates the asymptotic scaling behavior of  $j(x,t)$ , it is second order in fluctuations and will therefore have large corrections to scaling [18]. [The correlation function  $C_{jj}(x,t)$  decays so quickly with  $t$  that it is impossible to measure it for much larger  $t$  than shown in the figure.]

Since we have argued that the lack of scaling seen for  $C_{jj}(x,t)$  is a result of strong subleading corrections to its asymptotic behavior, it is reasonable to examine its spatial integral, i.e.,  $C_{JJ}$  at zero wave vector. An added motivation is that, if  $J(t) = \int dx j(x,t)$ , the Kubo formula obtains the conductivity as

$$\kappa = \frac{\beta^2}{L} \int_0^t dt' C_{JJ}(t'), \quad (7)$$

where  $\beta$  is the inverse temperature. From the definition of Eq. (2), the right-hand side of this equation is  $\beta^2 I(t)$ . We first show the results for  $I(t)$  for somewhat different conditions than those used so far in this paper.

Figure 8 is a log-log plot of  $I(t)/L^{1/3}$  as a function of  $t/L$  for different values of  $L$ . Unlike the data shown before this, the system does not have periodic boundary conditions, but is terminated by heat baths (both at unit temperature) at both ends. Also, the masses of the particles are not all equal, but alternate between 1 and 2.62 [19]. The figure shows a power law rise for  $I(t)$  with exponent  $t^{1/3}$ , which saturates at  $t \sim L$ . This is in accordance with the analytical prediction [7].

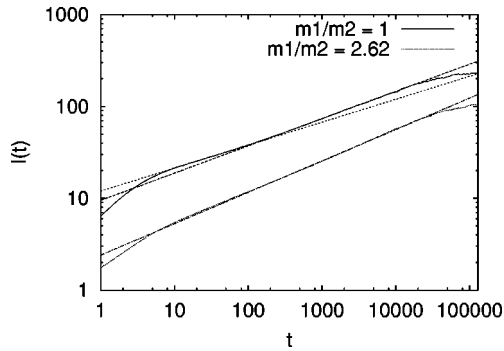


FIG. 9. Log-log plot of  $I(t)$  vs  $t$  for  $L=16384$ , where  $I(t)$  is defined in Eq. (2). All particles have unit mass. The slope shows an upward drift, from 0.24 (from  $t=10$  to  $t=100$ ) to 0.29 (from  $t=400$  to  $t=20000$ ), consistent with an eventual asymptotic slope of  $1/3$ . The figure also shows a similar plot for a chain whose masses alternate between 1 and 2.62, shifted downwards for clarity. A fit to a slope of 0.33 is shown; no upward (or downward) drift in the slope is seen. Periodic boundary conditions are used; over the range fitted, the results are the same with open boundary conditions.

There are a few damped oscillations at integer multiples of  $t \sim L$ , presumably corresponding to successive reflections from the ends of the system.

When all the particles in the chain are taken to have equal mass, there is a slight discrepancy from the analytical prediction. Figure 9 shows a log-log plot of  $I(t)$  for this case. The power law growth of  $I(t)$  has an exponent close to 0.25, but the saturation at  $t \sim L$  is still very clear. Taken at face value, this exponent would imply a conductivity exponent of  $\alpha=0.25$ , in contradiction to the analytical prediction. However, there are two reasons why this must be regarded simply as lack of complete convergence to the asymptotic form. First, as seen in this paper, the dynamics of the primitive hydrodynamic variables *do* agree with the analytical predictions; a fit with  $\delta x \sim t^{0.75}$  does not work. Second, and more directly, simulations on much larger systems, with  $L=16384$ , show an upward drift of the slope of  $\ln I(t)$  versus  $\ln t$ , towards  $1/3$ . No such drift of the slope is seen for the unequal mass case shown in Fig. 9. Note that there are also deviations from the asymptotic value of  $\alpha$  for the equal mass chain when the conductivity is measured directly [9], which was in fact the motivation for the detailed spatiotemporal measurements reported in this paper.

The most unusual result for the heat current autocorrelation function is obtained for  $I(t)$  for the case of periodic boundary conditions.

Figure 10 is a log-log plot of  $I(t)/L^{1/3}$  as a function of  $t/L$ . As was the case with heat baths at the ends,  $I(t)$  grows initially with the form  $\sim t^{1/3}$ , has damped oscillations at  $t \sim L$ , and saturates for large  $t$ . However, *unlike* the case with heat baths,  $I(t)$  continues to grow even after the oscillations set in, and the eventual asymptotic value scales as  $\approx L^{1/2}$ . In hindsight, this result is not inexplicable: without the heat baths, the dynamics are not cut off at the ends of the system, and the dynamic scaling exponent of  $z=3/2$  saturates the  $t^{1/3}$  growth at  $\sim L^{1/2}$ . Alternatively, the saturation of  $I(t)$  is set by the time a pulse takes to spread across the system rather

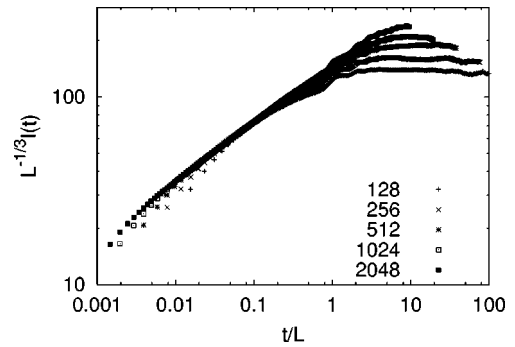


FIG. 10. Log-log plot of  $I(t)/L^{1/3}$  vs  $t/L$  for systems of different lengths, where  $I(t)$  is defined in Eq. (2). The particle masses alternate between 1 and 2.62. Periodic boundary conditions are used. For small  $t$ ,  $I(t)$  is the same as for open boundary conditions (shown in Fig. 8). However, beyond the oscillatory regime at  $t \sim O(L)$ ,  $I(t)$  keeps rising, and  $I(\infty)$  does not scale as  $\sim L^{1/3}$ .

than propagate across it. It is not clear exactly why the spreading cuts off the growth of  $I(t)$ , though from a scaling viewpoint one could argue that in the absence of the propagation time scale, the only possibility is  $L \sim t^{2/3}$ .

## VI. DISCUSSION

We have seen that the dynamics of the primitive hydrodynamic quantities, mass, momentum, and energy density, fit a scaling description with the predicted dynamic exponent. The scaling of the heat current autocorrelation function is more problematic. However, we have argued that this is to be expected, because the asymptotically dominant part of the current operator is bilinear in the primitive quantities and has a small bare value in the sense of the renormalization group compared to correction terms. The same slow convergence to asymptotic scaling that afflicts the heat current autocorrelation function has been noticed for the thermal conductivity and remarked on by various authors. However, the results for the primitive hydrodynamic quantities make it clear that this *is* indeed simply a case of slow convergence to the

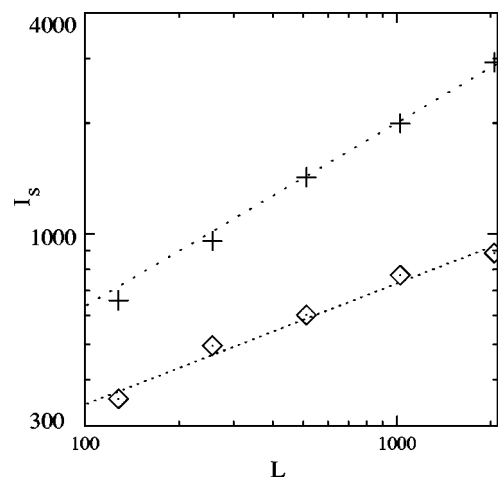


FIG. 11. Log-log plot of  $I(\infty)$  vs  $L$  for open and periodic boundary conditions. The straight lines show fits to  $\sim L^{1/3}$  and  $\sim L^{1/2}$ , respectively.

asymptotic limit rather than a discrepancy with the analytical prediction. Most remarkably, the large time limit of the spatiotemporal integral  $I(t)$  of the heat current autocorrelation function scales with  $L$  as  $\sim L^{1/3}$  for a system terminated with heat baths, and as  $\sim L^{1/2}$  for periodic boundary conditions (Fig. 11). This implies that in applying the Kubo formula to

systems with singular transport coefficients one must be careful about the boundary conditions being used.

#### ACKNOWLEDGMENTS

It is a pleasure to acknowledge useful discussions with Abhishek Dhar and Sriram Ramaswamy.

- 
- [1] Z. Rieder, J.L. Lebowitz, and E. Lieb, *J. Math. Phys.* **8**, 1073 (1967).
- [2] P. Grassberger and L. Yang, e-print cond-mat/0204247.
- [3] S.K. Bhatia and D. Nicholson, *Phys. Rev. Lett.* **90**, 016105 (2003).
- [4] T. Prosen and D.K. Campbell, *Phys. Rev. Lett.* **84**, 2857 (2000).
- [5] P. Grassberger, W. Nadler, and L. Yang, *Phys. Rev. Lett.* **89**, 180601 (2002).
- [6] G. Casati and T. Prosen, *Phys. Rev. E* **67**, 015203 (2003).
- [7] O. Narayan and S. Ramaswamy, *Phys. Rev. Lett.* **89**, 200601 (2002).
- [8] Ya.G. Sinai and N.I. Chernov, *Russ. Math. Surveys* **42**, 181 (1977).
- [9] J.M. Deutsch and O. Narayan, *Phys. Rev. E* **68**, 010201 (2003).
- [10] R. Kubo, *J. Phys. Soc. Jpn.* **12**, 570 (1957).
- [11] A. Casher and J.L. Lebowitz, *J. Math. Phys.* **12**, 1701 (1971); R.J. Rubin and W.L. Greer, *ibid.* **12**, 1686 (1971); A.J. O'Connor and J.L. Lebowitz, *ibid.* **15**, 692 (1974); H. Spohn and J.L. Lebowitz, *Commun. Math. Phys.* **54**, 97 (1977); H. Matsuda and K. Ishii, *Suppl. Prog. Theor. Phys.* **45**, 56 (1970).
- [12] A. Dhar, *Phys. Rev. Lett.* **86**, 5882 (2001).
- [13] S. Lepri, R. Livi, and A. Politi, *Europhys. Lett.* **43**, 271 (1998).
- [14] S. Lepri, R. Livi, and A. Politi, *Phys. Rev. Lett.* **78**, 1896 (1997); A.V. Savin, G.P. Tsironis, and A.V. Zolotaryuk, *ibid.* **88**, 154301 (2002); T. Hatano, *Phys. Rev. E* **59**, R1 (1999); A. Dhar, *Phys. Rev. Lett.* **86**, 3554 (2001).
- [15] D. Forster, *Hydrodynamic Fluctuations, Broken Symmetry, and Correlation Functions* (W. A. Benjamin, Reading, MA, 1975).
- [16] A small background has to be subtracted from  $C_{pp}$ , because for any given system the center of mass velocity is conserved. Thus, even though in the full canonical ensemble  $C_{pp}(x,t) = 0$  for large  $x$ , for zero center of mass velocity (for which the data are shown) there is a background value that ensures that  $\int dx C_{pp}(x,t) = 0$ .
- [17] J.A. McLennan, *Non-equilibrium Statistical Mechanics* (Prentice Hall, Engelwood Cliffs, NJ, 1989); see also F. Bonetto, J.L. Lebowitz, and L. Rey-Bellet, in *Mathematical Physics 2000*, edited by A. S. Fokas, A. Grigoryan, T. Kibble, and B. Zegarlinski (Imperial College Press, London, 2000), pp. 128–150.
- [18] One might alternatively try to obtain  $C_{jj}$  through the conservation law,  $C_{jj}(k,\omega) = (\omega^2/k^2)C_{qq}(k,\omega)$ . However this is a singular transformation, and relatively small corrections to scaling in  $C_{qq}$  can be accentuated in  $C_{jj}$ . We have verified that our numerical result for  $C_{jj}(k,\omega)$  is consistent with  $(\omega^2/k^2)C_{qq}(k,\omega)$ , but this does not lead to a good scaling form for  $C_{jj}$ .
- [19] In this case, one has to subtract  $(\bar{h}/\bar{m})g(x,t)$  from the energy current, where  $\bar{m}$  is the average mass density and  $g(x,t)$  is the momentum density. Thus the second term on the right-hand side of Eq. (5) is changed to  $(\bar{h}/\bar{m})\sum_i \delta(x-x_i)m_i v_i$ .